To cite this article：WEI Y W, ZHONG Q, WANG D Y. Ultimate strength prediction of I-core sandwich plate based on BP neural network [J/OL]. Chinese Journal of Ship Research, 2022, 17(2). http://www.ship-research.com/en/article/doi/10.19693/j.issn.1673-3185.02335.

DOI：10.19693/j.issn.1673-3185. 02335

Ultimate strength prediction of I-core sandwich plate based on BP neural network

*WEI Yuwen, ZHONG Qiang, WANG Deyu**

State Key Laboratory of Ocean Engineering, Shanghai Jiao Tong University, Shanghai 200240, China

Abstract: [**Objectives**] In view of the incomplete evaluation of the ultimate strength of I-core sandwich panels in the past, a BP artificial neural network method is proposed to quantitatively determine the influence of relevant parameters on the ultimate strength of I-core sandwich panels. [**Methods**] First, the ultimate strength of I-core sandwich panels under axial compression are investigated using the nonlinear finite element method. Second, a BP neural network is constructed to predict the ultimate strength of I-core sandwich panels with different face plate slenderness ratios between longitudinal webs, plate slenderness ratios of webs and column slenderness ratio of one longitudinal web. Finally, a formula for predicting the ultimate strength of I-core sandwich panels using the artificial neural network weight and bias method is proposed. [**Results**] The mean square error *MSE* and correlation coefficient *R* of ultimate strength prediction using the BP neural network method are 0.001 2 and 0.981 8 respectively. The proposed neural network model has good prediction accuracy, and the maximum error is less than 10%. [**Conclusions**] This study can provide references for the application of I-core sandwich panels in hull structures.

Key words: I-core sandwich panel; BP artificial neural network; ultimate strength; nonlinear finite element method; prediction

CLC number：U661.43

0 Introduction

An increasingly high standard for lightweight is raised in the design of modern ships to enable higher cargo loading and economical efficiency and obtain lighter hull structures on the premise of ensuring its due performance. Compared with the traditional stiffened panel, the I-core sandwich panel boasts excellent performance in fatigue resistance, crashworthiness, explosion impact resistance, vibration & noise reduction, etc. [1], thus attracting increasing attention in marine engineering. For example, metal sandwich structures have been applied to the antenna platform [2] of US Navy warships and the deck [3] of German ferries and cruise ships.

Some scholars have studied the strength of metal sandwich panels. For instance, Li et al. [4] used a nonlinear finite element (FE) method to compare the ultimate bearing capacity of I-core sandwich panels, U-core sandwich panels, and stiffened panels under uniaxial compression, providing a reference for the study of the in-plane bearing performance of metal sandwich panels. Hong et al. [5], resorting to a nonlinear FE method, simulated the ultimate bearing capacity of metal sandwich panels under combined loads, proving the better ultimate

Received：2021－03－30 **Accepted**：2021－05－25

Supported by: National Natural Science Foundation of China (51979163)

Authors：WEI Yuwen, female, born in 1998, master degree candidate. Research interest: ultimate strength of hull structure. E-mail: yuwenwei@sjtu.edu.cn

ZHONG Qiang, male, born in 1990, Ph.D. candidate. Research interest: ultimate strength of hull structure. E-mail: zhongqiang@sjtu.edu.cn

WANG Deyu, born in 1963, male, Ph.D., professor, doctoral supervisor. Research interests: structural mechanics of ship and marine engineering, structure optimization design and reliability analysis, and research on structural ultimate strength and testing technique. E-mail: dywang@sjtu.edu.cn

***Corresponding author**：WANG Deyu

bearing capacity of the designed metal sandwich panel than that of the traditional stiffened panel. Wang et al. [6] studied the in-plane connection structure of a sandwich panel from the aspects of modeling method, element type, mesh size, loading rate, initial defects, etc. Kozak [7] presented and compared the results of a test example and numerical simulation of a steel sandwich panel under an in-plane load, concluding that the cross-sectional geometric properties of the metal sandwich panel have a significant influence on its response under an in-plane load. Zhu et al. [8] proposed and verified a sub-model method for calculating the strength of the panel structure of the sandwich deck, the results of which confirmed its application in the accurate evaluation of structural strength characteristics.

Recent years have seen the widespread use of artificial neural networks in research areas such as structural reliability and strength prediction thanks to their high parallelism and fault tolerance. Mesbahi et al. [9] adopted an artificial neural network method to predict the formula for the ultimate strength of a stiffened plate under uniaxial compression and compared it with the existing empirical formula, finding that the result obtained by this method was more accurate than that obtained by the empirical formula. Wang et al. [10] used a neural network method to analyze the ultimate strength of a steel plate with random pitting damage, the result of which showed that the maximum relative error between the prediction result and the result of the FE analysis was less than 10%. Ahmadi et al. [11] used artificial neural network to predict the ultimate strength of a corroded steel plate with central longitudinal cracks and obtained the equation for ultimate strength prediction under different geometric and physical conditions. Tohidi et al. [12] built a new effective model with artificial neural networks to predict the buckling strength of semi-penetration bridges with an I-shaped cross-section, which proved that their method achieved a better estimation effect than that of the code.

To sum up, despite the progress in the research on the ultimate strength of I-core sandwich panels, relevant evaluation needs to be further improved, and relevant prediction formulas for the ultimate strength of such panels under different geometric conditions are still to be built. Therefore, focusing on the ultimate strength of I-core sandwich panels under different geometric conditions, this study calculates and analyzes the ultimate strength of I-core sandwich panels when they are under in-plane axial compressional loads with the nonlinear FE software ABAQUS and built the equation for ultimate strength prediction by an artificial BP neural network method to provide a reference for the application of I-core sandwich panels in hull structures.

1 Nonlinear FE analysis

1.1 Geometric sizes and material parameters

The structure of the I-core sandwich panel investigated in this study is shown in Fig. 1, which demonstrates that the panel is composed of upper and lower face plates and an I-shaped web. Its main parameters include thickness t_p of the upper and lower face plates, web thickness t_w, web height h_w, web spacing d_w, width c of the I-core sandwich plate, beam spacing a, buckling half-wave number e, and yield strength σ_Y, as shown in Table 1. References [13-16] are available for the size selection ranges. The Young's modulus E of all FE model materials is 206 GPa, and their Poisson's ratio μ = 0.3, with no regard to the effect of material hardening. In the subsequent analysis, three materials of different yield strengths, which are 235, 315, and 390 MPa respectively, are selected.

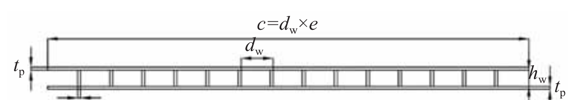

(a) Cross-section

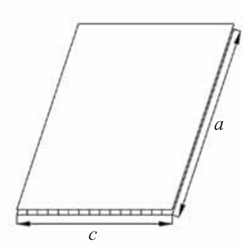

(b) Whole model

Fig. 1 Structure of I-core sandwich panel

Table 1 Geometric sizes and material parameters of I-core sandwich panel

Parameter	Value
Thickness t_p of upper and lower panels/mm	2，3，4
Web thickness t_w/mm	2，4，6，8
Web height h_w/mm	40，60，80
Web spacing d_w/mm	80，120，160
Beam spacing a/mm	2 500，3 000，3 500
Buckling half-wave number e	15
Yield strength σ_Y/MPa	235，315，390

1.2 Boundary conditions

The ultimate strength of the I-core sandwich panel structure is investigated within the ranges of three models (Figs. 2-4): longitudinal three-span model (with actual strong members), longitudinal 1/2+1+1/2 span model (with boundary conditions instead of strong beams), and longitudinal single-span model (with boundary conditions instead of strong members).

The sizes of the strong beam of a full-scale ship are selected for the strong beam of the longitudinal three-span model (with actual strong members) (Fig. 2), i.e., a web height of 380 mm, a web thickness of 12 mm, a face plate width of 160 mm, and a face plate thickness of 14 mm. The boundary conditions are presented in Table 2, where U_x, U_y, and U_z are linear displacements and R_x, R_y, and R_z are angular displacements. The longitudinal boundaries of the model are A1-A2, A1'-A2', B1-B2, and B1'- B2' respectively. The transverse boundaries of the face plate of the strong beam are C1-D1, C2-D2, G1-H1, and G2-H2, and the transverse boundaries of the web of the strong beam are E1-F1, E2-F2, J1-K1, and J2-K2.

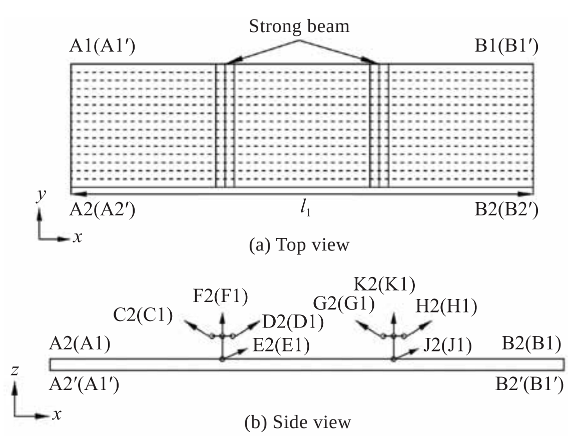

Fig. 2 Longitudinal three-span model (with actual strong members)

Table 2 Boundary conditions of longitudinal three-span model (with actual strong members)

Application range	U_x	U_y	U_z	R_x	R_y	R_z
A1-B1, A1'-B1', A2-B2, A2'-B2'			0		0	0
A1-A2, A1'-A2'	Displacement load	0	0	0		0
B1-B2, B1'-B2'	0	0	0	0		0
C1-D1, C2-D2, E1-F1, E2-F2, G1-H1, G2-H2, J1-K1, J2-K2			0			

The longitudinal 1/2+1+1/2 span model (with boundary conditions instead of strong beams) is shown in Fig. 3, and its boundary conditions are presented in Table 3. The model draws on the boundary condition analysis method presented in Reference [17], with the loading edge adopting symmetrical boundary conditions and the constraints on the vertical displacement and the rotation angle in the y direction replacing the actual strong members. In this figure, K1-K2 and L1-L2 represent the locations of the strong beams.

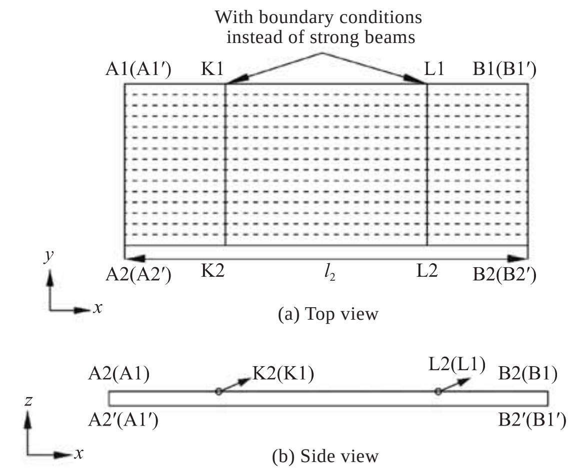

Fig. 3 Longitudinal 1/2+1+1/2 span model (with boundary conditions instead of strong beams)

Table 3 Boundary conditions of longitudinal 1/2+1+1/2 span model (with boundary conditions instead of strong beams)

Application range	U_x	U_y	U_z	R_x	R_y	R_z
A1-B1, A1'-B1', A2-B2, A2'-B2'			0		0	0
A1-A2, A1'-A2'	Displacement load				0	0
B1-B2, B1'-B2'	0				0	0
K1-K2, L1-L2			0		0	

The longitudinal single-span model (with boundary conditions instead of strong members) is shown in Fig. 4, and its boundary conditions are presented in Table 4.

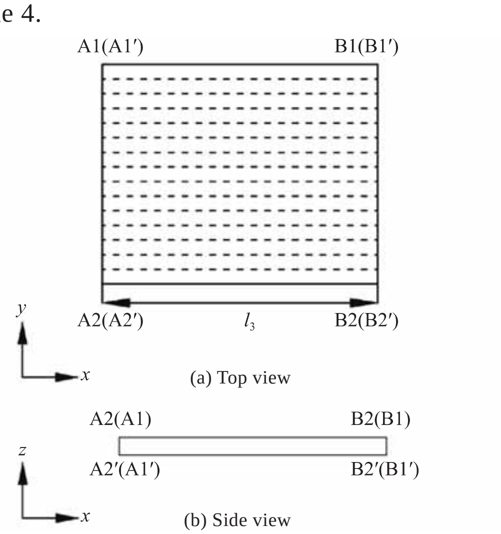

Fig. 4 Longitudinal single-span model (with boundary conditions instead of strong members)

Table 4 Boundary conditions of longitudinal single-span model (with boundary conditions instead of strong members)

Application range	U_x	U_y	U_z	R_x	R_y	R_z
A1-B1, A1'-B1', A2-B2, A2'-B2'			0		0	0
A1-A2, A1'-A2'	Displacement load	0	0	0		0
B1-B2, B1'-B2'	0	0	0	0		0

Within the ranges of the three models, the load-deformation curves obtained by FE analysis are presented in Fig. 5. The load value corresponding to the highest point of a load-deformation curve is considered as the ultimate load, and the average stress obtained by dividing the ultimate load by the cross-section area of the I-core sandwich panel is defined as the ultimate strength σ_u. In this figure, δ/L represents the ratio of the deformation length δ to the length L of the I-core sandwich panel, σ_u/σ_Y is the ratio of the ultimate strength σ_u to the yield strength σ_Y, where L is l_1, l_2, and l_3 in Figs. 2, 3, and 4 respectively. Fig. 5 indicates that the σ_u/σ_Y within the ranges of two models—the longitudinal three-span model (with actual strong members) and the longitudinal 1/2+1+1/2 span model (with boundary conditions instead of strong beams) is almost consistent. The range of the model-longitudinal 1/2+1+1/2 span model (with boundary conditions instead of strong members) is selected as the calculation model of this study under comprehensive consideration of calculation accuracy and cost.

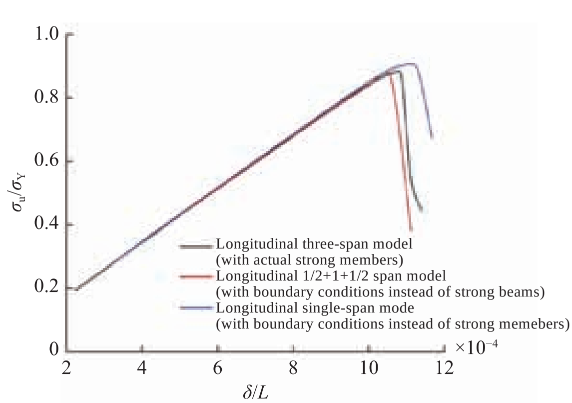

Fig. 5 Comparison of load-deformation curves of I-core sandwich panel under axial compression with the ranges of different models

1.3 Initial geometric defects

Structures are all exposed to some initial defects inevitably, which, however, significantly affect their failure mode and ultimate bearing capacity. The initial deformation of the I-core sandwich panel is given in the following three forms: the initial deformation of upper and lower face plate elements, that of core web elements, and that of the whole structure. In this study, the MSC Patran software is adopted to add initial defects to the stiffened panel model. Specifically, the initial deformation shown in Eq. (1) is applied to the upper face plate, that shown in Eq.(2) is applied to the lower face plate, that shown in Eq. (3) is applied to the core web, and that shown in Eq. (4) is applied to the whole structure.

$$w_{\mathrm{opt}} = A_0 \sin\left(\frac{e\pi x}{a}\right)\sin\left(\frac{\pi y}{d_{\mathrm{w}}}\right) \tag{1}$$

$$w_{\mathrm{opb}} = -A_0 \sin\left(\frac{e\pi x}{a}\right)\sin\left(\frac{\pi y}{d_{\mathrm{w}}}\right) \tag{2}$$

$$w_{\mathrm{oc}} = \frac{h_{\mathrm{w}}}{d_{\mathrm{w}}} \times A_0 \sin\left(\frac{e\pi x}{a}\right)\sin\left(\frac{\pi z}{h_{\mathrm{w}}}\right) \tag{3}$$

$$w_{\mathrm{og}} = B_0 \sin\left(\frac{\pi x}{a}\right) \tag{4}$$

In these equations, A_0=0.1$\beta^2 t_p$, where $\beta = \frac{b_w}{t_p}\sqrt{\frac{\sigma_Y}{E}}$, is the flexibility coefficient of the panel; B_0=0.001 5a; e is the buckling half-wave number and is defined as the smallest integer that meets the requirement $a/d_w \leqslant \sqrt{e(e+1)}$.

1.4 Convergence analysis

As for the mesh size, 1/8, 1/4, 1/2, and one time the height of the core web are selected for analysis, with the numerical results of the I-core sandwich panel under different mesh densities presented in Table 5.

Table 5 Numerical results of I-core sandwich panel with different mesh densities

Mesh size/mm	σ_u /MPa
1/8h_w	183.671 7
1/4h_w	184.319 9
1/2h_w	189.535 6
h_w	207.345 3

The calculation results in the table indicate that a reasonable result can already be obtained when the mesh size is 1/4h_w compared with that in the case of a higher mesh density. Therefore, the subsequent FE analysis adopts the mesh size of 1/4h_w.

1.5 Simulation technique and result verification

The commercial software ABAQUS is adopted for nonlinear FE analysis, the S4R four-node shell element is used for modeling, and the Riks method is employed for calculation and analysis. As one of the iterative control methods that perform numerical calculations most stably, efficiently, and reliably for nonlinear analysis of structures at the moment, the Riks method can well analyze the nonlinear pre- and post-buckling of structures and track the buckling path.

Before massive FE analysis of ultimate strength, simulation calculation is performed according to the existing test results of I-core sandwich panel structures [7] to verify the accuracy of the nonlinear FE technique used in this study and the calculation results. The sizes of the simulation model are as follows: The length and width of the I-core sandwich panel are 3 000 and 500 mm, respectively; the thickness of the upper and lower face plates is 3 mm, the height of the core web is 60 mm; the core web spacing is 80 mm. An ideal elastic-plastic material with a yield strength of 235 MPa is adopted, and the initial geometric defects described in Section 1.3 are added to it. Under an in-plane load parallel to the direction of the core web, the load-end shortening curves of the I-core sandwich panel are shown in Fig. 6. The peak strength error is about 3.67%, and the end shortening error is about 0.007 5%. The FE simulation result is in good agreement with the curve in Reference [7], and the failure mode is also similar to the test result (Fig. 7). Therefore, the FE analysis method adopted here is applicable to and reasonable for the subsequent simulation calculation.

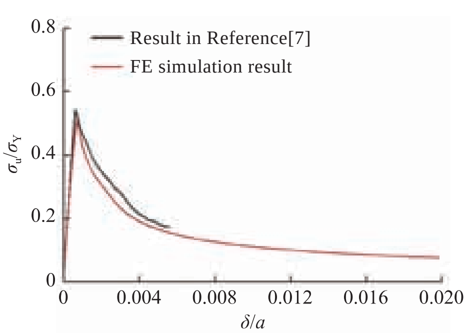

Fig. 6 Comparison of load-deformation curves of I-core sandwich panel under axial compression

(a) Model test[7] (b) FE simulation

Fig. 7 Comparison of failure mode between model test and FE simulation

2 BP neural network structure

Artificial neural networks are well equipped for the prediction of the output of complex systems. BP neural networks, also known as back-propagation neural networks, are a widely used neural network model featuring high nonlinearity and generalization. A BP neural network can be divided into three layers: input layer, hidden layer, and output layer, with each containing multiple neurons. A BP neural network processes input data through multi-layer neurons: when a learning mode network is given, the activation values of the neurons are transmitted from the input layer to the output layer via the hidden layer, and the neurons at the output layer output respond corresponding to the neurons at the input layer; for a smaller error between the actual output value and the expected one, the error signal is transmitted from the output layer to the hidden layer and then to the input layer to adjust the connection weight, thereby ensuring a small error between the predicted value output after training and the desired predicted value.

The input layer of the neural network structure adopted here contains three neurons—the face plate slenderness ratio β_p, web slenderness ratio β_w, and slenderness ratio λ of the column with one web, and they are respectively expressed by the following Eqs.:

$$\beta_p = \frac{b_w}{t_p}\sqrt{\frac{\sigma_Y}{E}} \tag{5}$$

$$\beta_w = \frac{h_w}{t_w}\sqrt{\frac{\sigma_Y}{E}} \tag{6}$$

$$\lambda = \frac{a}{\pi r}\sqrt{\sigma_Y/E} \tag{7}$$

$$r = \sqrt{I/A} \tag{8}$$

where I represents the moment of inertia of the cross-section containing one web and the related face plates; A is the area of the cross-section containing one web and the related face plates.

The output layer contains one neuron that represents the ratio of ultimate strength to yield strength σ_u/σ_Y. The commonly used training functions in Matlab include Trainlm, Traingd, Traingdm, Traingda, and Traingdx. To select the proper training function, this paper, by inputting training samples, decides that the hidden layer contains nine neurons, the maximum number of training is 1 000, and the training accuracy is 0.002 0. Then, the training results obtained with different training functions are compared to select the optimal training function, as shown in Table 6.

The iteration accuracy in Table 6 is the mean square error after the iterations end. And Trainlm is the optimal training function in terms of both the number of iterations and iteration accuracy.

One or two hidden layers and the grids under different numbers of neurons are adopted for training, and the results are shown in Table 7. Comprehensive consideration of the number of iterations and iteration accuracy reveals that among the 17 training models, the optimal one is the one with a single hidden layer that has nine neurons. Therefore, one hidden layer with nine neurons is adopted for this study.

Table 6 Performance comparison of different training functions

Function	Algorithm	Number of iterations	Iteration accuracy
Trainlm	Levenberg-Marquardt method	25	0.002 0
Traingd	Gradient descent method	1 000	0.012 1
Traingdm	Gradient descent method with momentum factors	1 000	0.034 7
Traingda	Gradient descent mehtod with self-adaptive learning rate	1 000	0.005 9
Traingdx	Gradient descent mehtod with self-adaptive learning rate and momentum factors	1 000	0.010 1

Table 7 Performance comparison of different numbers of hidden layers and neurons

Number of neurons at Hidden Layer 1	Number of neurons at Hidden Layer 2	Number of iterations	Iteration accuracy
3	0	1 000	0.002 2
4	0	1 000	0.003 4
5	0	1 000	0.002 5
6	0	1 000	0.002 7
7	0	235	0.002 0
8	0	360	0.002 0
9	0	25	0.002 0
10	0	72	0.001 9
11	0	133	0.002 0
12	0	71	0.001 9
3	3	71	0.002 0
3	4	150	0.002 0
3	5	153	0.001 9
3	6	192	0.001 9
3	7	52	0.002 0
3	8	289	0.002 0
3	9	85	0.002 0

The topological structure of the three-layer BP neural network adopted in this study is 3-9-1, as shown in Fig. 8. To be specific, the layers are connected by weight w and bias b, with no connection among the neurons at the same layer. The Trainlm function is selected for training, with a maximum number of training steps of 1 000 and a target error of 0.002 0.

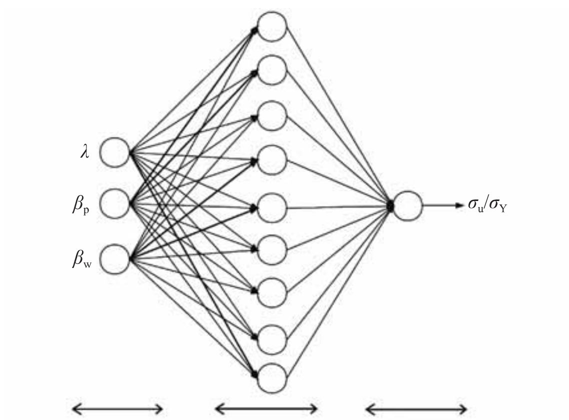

Fig. 8 Structure of BP neural network for predicting the ratio of ultimate strength to yield strength of I-core sandwich panel

The logsig function is adopted as the transfer function of the hidden layer, with its basic expression presented as

$$f(x)=\frac{1}{1+\exp(-x)} \tag{9}$$

The input of the j-th neuron at the hidden layer is

$$yinput_j=\left[\sum_{i=1}^{n} w_{ij}x_i\right]+b_j \tag{10}$$

where w_{ij} is the weight between the input layer and the hidden layer; b_j is the bias between the input layer and the hidden layer; n is the number of neurons at the input layer; x_i is the value of the i-th input neuron. The output of the j-th neuron at the hidden layer is

$$u_j=\frac{1}{1+\exp(-yinput_j)} \tag{11}$$

The purelin function is adopted as the transfer function of the output layer, with its basic expression presented as

$$f(x)=x \tag{12}$$

The input of the output layer is

$$yinput_{\mathrm{p}}=\left[\sum_{k=1}^{m} w_{jk}u_j\right]+b_k \tag{13}$$

where w_{jk} and b_k are the weight and bias between the hidden layer and the output layer respectively; m is the number of neurons at the hidden layer.

The output of the output layer is

$$youtput_{\mathrm{o}} = youtput_{\mathrm{p}} \tag{14}$$

As the error signal back-propagates, the weight is corrected layer by layer according to the error backward, and the network is updated through the constant updating of the weight:

$$w(t+1) = w(t) + \eta error(t) youtput(t) \tag{15}$$

$$b(t+1) = b(t) + \eta error(t) \tag{16}$$

where t is the number of iterations; $error$ is the difference between the expected output and the actual one; η is the learning rate; $youtput$ is the output of the neuron.

To measure the accuracy of the operation results of the BP neural network, this study adopts the mean square error MSE and correlation coefficient R to evaluate the operation results:

$$MSE = \frac{\sum_{i=1}^{q} (youtput_{\mathrm{predicted}} - youtput_{\mathrm{desired}})^2}{q} \tag{17}$$

$$R = 1 - \frac{\sum_{i=1}^{q} (youtput_{\mathrm{predicted}} - youtput_{\mathrm{desired}})}{\sum_{i=1}^{q} (youtput_{\mathrm{predicted}} - \overline{youtput}_{\mathrm{desired}})} \tag{18}$$

where q is the number of data; $youtput_{\mathrm{predicted}}$ is the output predicted value; $youtput_{\mathrm{desired}}$ is the desired predicted value. The correlation coefficient R represents the degree of the correlation between the predicted value and the actual one, and the R value closer to 1 indicates higher prediction accuracy of the network. In this study, 252 groups of datasets are adopted as the database for the operation of the BP neural network, with some data listed in Table 8.

Table 8 FE simulation results

No.	λ	β_{p}	β_{w}	$\sigma_{\mathrm{u}}/\sigma_{\mathrm{Y}}$	No.	λ	β_{p}	β_{w}	$\sigma_{\mathrm{u}}/\sigma_{\mathrm{Y}}$
1	6.370 6	1.351 0	0.675 5	0.880 7	33	3.185 3	0.675 5	1.351 0	0.954 9
2	6.715 4	1.351 0	0.337 8	0.892 1	34	3.357 7	0.675 5	0.675 5	0.992 9
3	7.003 7	1.351 0	0.225 2	0.850 4	35	3.501 9	0.675 5	0.450 3	0.996 8
4	7.249 1	1.351 0	0.168 9	0.795 4	36	3.624 5	0.675 5	0.337 8	0.996 7
5	6.099 1	0.900 7	0.675 5	0.944 7	37	6.240 0	2.026 5	0.675 5	0.581 4
6	6.352 8	0.900 7	0.337 8	0.982 0	38	6.492 9	2.026 5	0.337 8	0.604 5
7	6.576 6	0.900 7	0.225 2	0.981 9	39	6.715 4	2.026 5	0.225 2	0.585 9
8	6.775 9	0.900 7	0.168 9	0.976 4	40	6.913 0	2.026 5	0.168 9	0.565 0
9	5.894 5	0.675 5	0.675 5	0.953 1	41	6.006 7	1.351 0	0.675 5	0.710 8
10	6.094 4	0.675 5	0.337 8	0.996 0	42	6.187 3	1.351 0	0.337 8	0.788 9
11	6.276 1	0.675 5	0.225 2	0.997 4	43	6.352 8	1.351 0	0.225 2	0.776 7
12	6.442 2	0.675 5	0.168 9	0.996 9	44	6.505 0	1.351 0	0.168 9	0.760 1
13	4.431 3	1.351 0	1.013 3	0.861 6	45	5.823 3	1.013 3	0.675 5	0.751 6
14	4.731 1	1.351 0	0.506 6	0.872 9	46	5.963 4	1.013 3	0.337 8	0.882 1
15	4.965 2	1.351 0	0.337 8	0.856 0	47	6.094 4	1.013 3	0.225 2	0.891 3
16	5.153 8	1.351 0	0.253 3	0.830 8	48	6.217 4	1.013 3	0.168 9	0.883 9
17	4.247 1	0.900 7	1.013 3	0.928 1	49	4.311 5	2.026 5	1.013 3	0.669 0
18	4.476 9	0.900 7	0.506 6	0.974 1	50	4.540 3	2.026 5	0.506 6	0.714 0
19	4.669 2	0.900 7	0.337 8	0.974 6	51	4.731 1	2.026 5	0.337 8	0.703 6
20	4.832 7	0.900 7	0.253 3	0.970 2	52	4.893 0	2.026 5	0.253 3	0.685 6
21	4.119 3	0.675 5	1.013 3	0.942 9	53	4.160 0	1.351 0	1.013 3	0.801 5
22	4.304 9	0.675 5	0.506 6	0.992 0	54	4.328 6	1.351 0	0.506 6	0.852 6
23	4.466 4	0.675 5	0.337 8	0.995 1	55	4.476 9	1.351 0	0.337 8	0.851 7
24	4.608 4	0.675 5	0.253 3	0.992 0	56	4.608 6	1.351 0	0.253 3	0.837 3
25	3.429 3	1.351 0	1.351 0	0.900 3	57	4.051 0	1.013 3	1.013 3	0.847 2
26	3.692 6	1.351 0	0.675 5	0.918 6	58	4.184 2	1.013 3	0.506 6	0.907 1
27	3.886 9	1.351 0	0.450 3	0.902 4	59	4.304 9	1.013 3	0.337 8	0.913 6
28	4.036 6	1.351 0	0.337 8	0.883 4	60	4.414 9	1.013 3	0.253 3	0.909 0
29	3.282 4	0.900 7	1.351 0	0.943 7	61	3.319 0	2.026 5	1.351 0	0.714 7
30	3.491 5	0.900 7	0.675 5	0.980 0	62	3.527 0	2.026 5	0.675 5	0.775 6
31	3.658 4	0.900 7	0.450 3	0.979 4	63	3.692 6	2.026 5	0.450 3	0.783 6
32	3.795 1	0.900 7	0.337 8	0.969 3	64	3.828 0	2.026 5	0.337 8	0.777 2

Before the analysis, the initial input data need to be normalized to eliminate the influence of dimension due to the significant difference in the value range of input data. In this study, the database is normalized to the extent that it is within the interval [0, 1]:

$$x_n' = \frac{x_n - \min(D)}{\max(D) - \min(D)} \tag{19}$$

where D represents a group of series in the dataset; $\min(D)$ is the minimum value and $\max(D)$ is the maximum value in this group of series; x_n is the value to be normalized; x_n' is the normalized value.

The datasets in the database are randomly divided into training sets, validation sets, and testing sets. They account for 70%, 15%, and 15% of the total datasets, respectively, and are independent of each other. Among them, the training sets are used for model training; the validation sets are for the validation of the trained model to test whether the model performs well on new data and thereby to facilitate the adjustment of the hyper-parameters of the model, and the testing sets are for the final evaluation of the neural network model.

3 Results and discussions

3.1 Numerical results

Table 8 lists the σ_u/σ_Y of some structures in 252 I-core sandwich panels under an in-plane axial compressional load obtained by FE simulation. The table reveals that regarding all the I-core sandwich panels, their face plate slenderness ratio β_p is between 0.67 and 3.51, their web slenderness ratio β_w is between 0.16 and 1.76, and their column slenderness ratio λ is between 3.00 and 9.40.

3.2 Operation results of BP neural network

As described in Section 2, a topological structure of 3-9-1 is designed for the three-layer BP neural network, and the ultimate strength of I-core sandwich panels with different β_p, β_w, and λ under an in-plane axial compressional load is predicted. Figs. 9-12 present the correlation between the expected value and the predicted one of σ_u/σ_Y in the training sets, validation sets, testing sets, and all the sets respectively. These figures show that all the data are located near the $x = y$ curve. Specifically, the correlation coefficient R in the testing sets is 0.981 8, suggesting high correlation and coincidence.

Fig. 13 shows the expected and predicted values of σ_u/σ_Y in the testing sets and the error between them. Among the 38 groups of data in the testing sets, the maximum error between the expected and predicted values is 0.082 2, and the mean square error *MSE* is 0.001 2. This result proves that the BP neural network structure adopted in this study delivers favorable prediction performance.

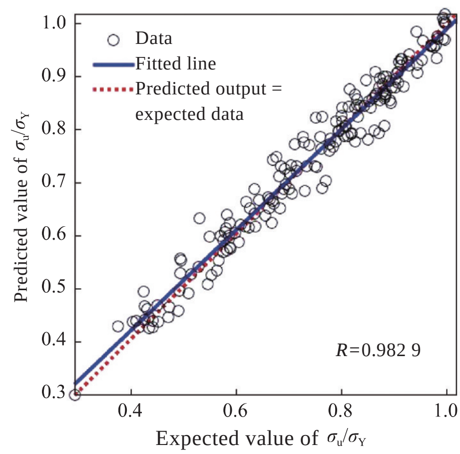

Fig. 9 Correlation between the expected data and predicted outputs of σ_u/σ_Y in training sets

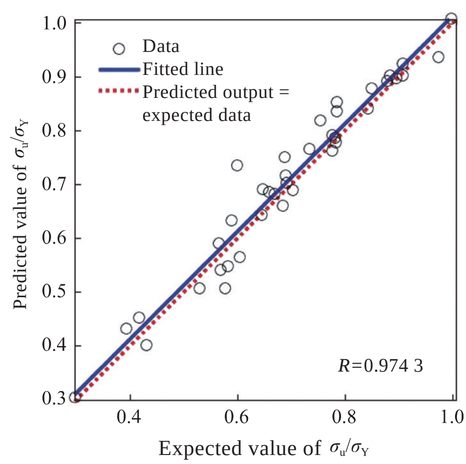

Fig. 10 Correlation between the expected data and predicted outputs of σ_u/σ_Y in validation sets

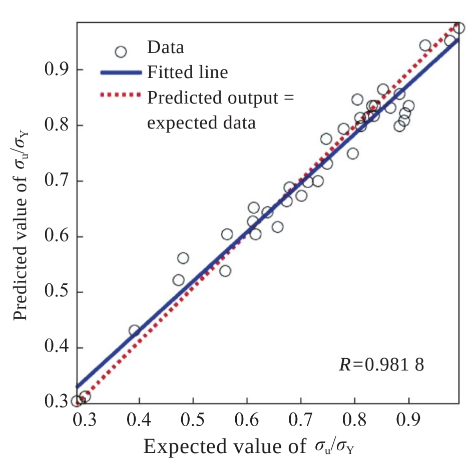

Fig. 11 Correlation between the expected data and predicted outputs of σ_u/σ_Y in testing sets

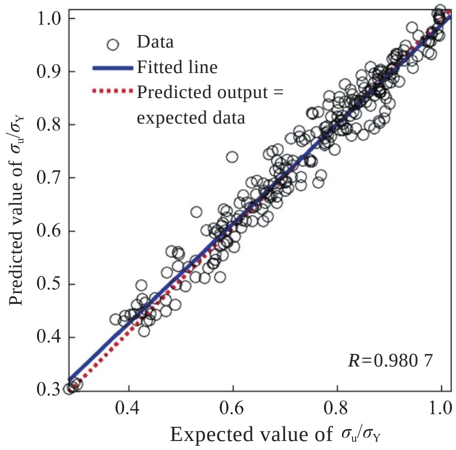

Fig. 12 Correlation between the expected data and predicted outputs of σ_u/σ_Y in all the sets

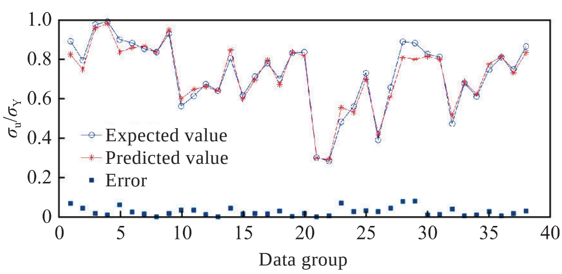

Fig. 13 Error between the expected data and predicted outputs of σ_u/σ_Y in testing sets

An equation for predicting the ultimate strength of I-core sandwich panels with different β_p, β_w, and λ under an in-plane axial compressional load is put forward on the basis of the weight and error of the BP neural network.

$$\frac{\sigma_u}{\sigma_Y}=\left[\sum_{j=1}^{9} w_{jk}x_j\right]+b_k \tag{20}$$

where

$$x_j=\frac{1}{1+\exp(-G)} \tag{21}$$

in which G can be expressed by the following formula:

$$G=\left[\sum_{i=1}^{3} w_{ij}x_i\right]+b_j \tag{22}$$

The values of the parameters in Eqs. (20) to (22) are presented in Table 9, where k, j, and i represent the k-th, j-th, and i-th neuron at the output layer, hidden layer, and input layer respectively.

3.3 Verification of BP neural network model

Table 10 lists the geometric sizes of 20 I-core sandwich panel structures used to test the BP neural network model and the ultimate strength of these structures under an in-plane axial compressional load. The β_p, β_w, and λ of these metal sandwich panel structures are all within the ranges described in

Table 9 Values of parameters in ultimate strength prediction equation for I-core sandwich panels

k	j	i	w_{ij}	b_j	w_{jk}	b_k
1	1	1	15.787 83			
		2	−1.317 5	−8.060 5	−1.134 29	3.508 448
		3	1.242 68			
	2	1	−3.184 67			
		2	−12.944 9	14.235 29	0.202 705	
		3	−1.725 95			
	3	1	−5.953 61			
		2	11.236 42	1.084 991	−0.376 16	
		3	0.961 726			
	4	1	29.143 18			
		2	−3.361 12	−14.747 2	0.815 201	
		3	4.365 897			
	5	1	0.309 728			
		2	15.531 94	−3.401 43	−0.135 02	
		3	−12.604 4			
	6	1	−1.301 16			
		2	−6.731 54	−1.886 73	−2.492 59	
		3	8.029 399			
	7	1	6.911 944			
		2	12.653 35	−9.691 39	−0.172 38	
		3	6.526 226			
	8	1	2.203 471			
		2	6.820 759	1.637 875	−2.538 26	
		3	−7.541 44			
	9	1	−6.343 71			
		2	−13.337 1	5.825 758	0.036 682	
		3	−3.522 82			

Section 3.1.

The BP neural network built above is applied to predicting the ultimate strength of the I-core sandwich panels in Table 10 under an in-plane axial compressional load, and the results are presented in Fig. 14. This figure shows that the maximum error between the expected value and the predicted one is 0.086 1 and the mean square error MSE is 0.001 1, proving that favorable prediction results are achieved.

3.4 Sensitivity analysis

As sensitivity analysis needs to be conducted to evaluate the influence of the three variable parameters of the input layer on the output, and the sensitivity analysis method based on connection weights

Table 10 Parameters of I-core sandwich panels

No.	λ	β_p	β_w	σ_u/σ_Y
1	4.962 2	0.965 0	0.562 9	0.921 4
2	5.131 2	0.965 0	0.337 8	0.949 6
3	5.283 2	0.965 0	0.241 3	0.945 0
4	5.829 0	2.346 2	0.651 7	0.502 8
5	6.013 8	2.346 2	0.391 0	0.512 9
6	6.180 7	2.346 2	0.279 3	0.502 2
7	5.638 6	1.675 9	0.651 7	0.618 2
8	5.779 2	1.675 9	0.391 0	0.648 9
9	5.909 6	1.675 9	0.279 3	0.647 4
10	4.927 6	1.740 4	1.015 3	0.675 8
11	5.174 9	1.740 4	0.609 2	0.679 8
12	5.380 0	1.740 4	0.435 1	0.666 9
13	4.943 5	1.243 2	0.609 2	0.852 1
14	5.116 1	1.243 2	0.435 1	0.851 7
15	3.713 2	2.026 5	0.788 1	0.681 2
16	3.859 8	2.026 5	0.472 9	0.705 2
17	3.987 5	2.026 5	0.337 8	0.709 6
18	3.596 2	1.447 5	0.788 1	0.801 5
19	3.710 2	1.447 5	0.472 9	0.829 8
20	3.813 2	1.447 5	0.337 8	0.834 1

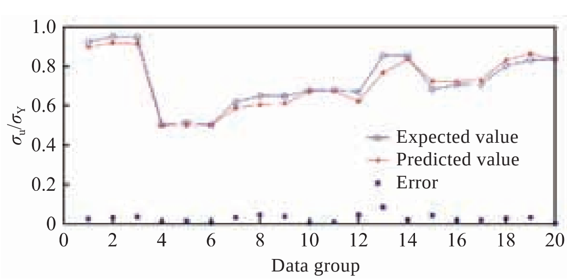

Fig. 14 Error between expected data and predicted outputs of σ_u/σ_Y

is adopted [18]. The degree of the influence of the input variables on the output variables can be expressed by the following formula

$$Q_i = \frac{\sum_{j=1}^{m}[|w_{ij}\cdot w_{jk}|/\sum_{i=1}^{n}(|w_{ij}\cdot w_{jk}|)]}{\sum_{i=1}^{n}\sum_{j=1}^{m}[|w_{ij}\cdot w_{jk}|/\sum_{i=1}^{n}(|w_{ij}\cdot w_{jk}|)]} \tag{23}$$

The relative degrees of the influences of the input variable parameters β_p, β_w, and λ on the σ_u/σ_Y of the I-core sandwich panel structures under an axial in-plane compressional load are thereby obtained and shown in Fig. 15. Specifically, β_w reports the relatively lowest degree of influence of 26.87% while β_p has the relatively highest degree of influence of 39.99%.

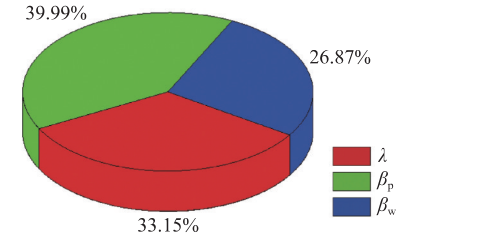

Fig. 15 Relative importance of the input variables β_p, β_w, and λ on the response variable of σ_u/σ_Y of I-core sandwich panels

4 Conclusions

In this study, the ultimate strength of 252 I-core sandwich panel models under an in-plane axial compressional load is calculated and analyzed with the nonlinear FE software ABAQUS, and an equation for ultimate strength prediction is built by an artificial BP neural network method. The following conclusions are reached for the sizes of the examples calculated in this study:

1) Compared with the results of nonlinear FE calculation, the ultimate strength predicted by the BP neural network method has a mean square error *MSE* of 0.001 2, a correlation coefficient *R* of 0.981 8 respectively, and a maximum error of no more than 10%, indicating favorable prediction performance.

2) The web slenderness ratio β_w has the relatively lowest degree of influence on the I-core sandwich panel structures, is 26.87%, whereas β_p has the relatively highest degree of influence, is 39.99%.

3) An equation for predicting the ultimate strength of I-core sandwich panels under an in-plane axial compressional load is put forward on the basis of the weights and biases of the designed neural network structure, and it can provide a reference for the application of I-core sandwich panels in hull structures.

References

[1] CHEN Y K, HE S T, LIU J, et al. Application and prospect of steel sandwich panels in warships [J]. Chinese Journal of Ship Research, 2013, 8 (6): 6−13 (in Chinese).

[2] LI Z, GOBBI S L. Laser welding for lightweight structures [J]. Journal of Materials Processing Technology, 1997,70 (1): 137−144.

[3] NOURY P, HAYMAN B, MCGEORGE D, et al. Lightweight construction for advanced shipbuilding-recent development [R]. [S.l.]: Det Norske Veritas, 2002.

[4] LI Z J, HUANG L, ZHAO N, et al. Ultimate bearing capacity for steel sandwich panels under uniaxial com-

pression [J]. Chinese Journal of Ship Research, 2020, 15 (4): 53−58 (in Chinese).
[5] HONG T T, TIAN A L, PAN K H. Post-buckling strength analysis of corrugated core sandwich panel under combined compression loading [J]. Ship Science and Technology, 2018, 40 (9): 43−47 (in Chinese).
[6] WANG G, HU Z W, WANG Z L, et al. Numerical simulation technology for mechanical property analysis of sandwich panel connections in plane [J]. Ship Science and Technology, 2014, 36 (6): 54−59 (in Chinese).
[7] KOZAK J. Problems of strength modeling of steel sandwich panels under in-plane load [J]. Polish Maritime Research, 2006 (Supp 1): 9−12.
[8] ZHU Y, CHENG Y S, LIU J. Sub-model method for strength calculation of a laser-welded steel sandwich panel structure [J]. Journal of Ship Mechanics, 2014, 18 (10): 1228−1236 (in Chinese).
[9] MESBAHI E, PU Y C. Application of ANN-based response surface method to prediction of ultimate strength of stiffened panels [J]. Journal of Structural Engineering, 2008, 134 (10): 1649−1656.
[10] WANG R H, ZHAO S S. Ultimate strength prediction of steel plate with random pitting corrosion damage[J]. Engineering Mechanics, 2018, 35 (12): 248−256 (in Chinese).
[11] AHMADI F, RANJI A R, NOWRUZI H. Ultimate strength prediction of corroded plates with center-longitudinal crack using FEM and ANN [J]. Ocean Engineering, 2020, 206: 107281.
[12] TOHIDI S, SHARIFI Y. A new predictive model for restrained distortional buckling strength of half-through bridge girders using artificial neural network [J]. KSCEJournal of Civil Engineering, 2016, 20 (4): 1392−1403.
[13] KOZAK J. Fatigue tests of steel sandwich panel [M]. England: Marine and Maritime, 2003: 59−68.
[14] METSCHKOW B. Sandwich panels in shipbuilding [J]. Polish Maritime Research, 2006 (Supp 1): 5−8.
[15] BORONSKI D, KOZAK J. Research on deformations of laser-welded joint of a steel sandwich structure model [J]. Polish Maritime Research, 2004, 11 (2): 3−8.
[16] GAO C, LIU W F, QIU W Q, et al. Numerical vibration analysis of steel sandwich plates with I-shaped cores [J]. Noise and Vibration Control, 2018, 38 (4): 76−80, 179 (in Chinese).
[17] PAIK J K, KIM B J, SEO J W. Methods for ultimate limit state assessment of ships and ship-shaped offshore structures: Part II stiffened panels [J]. Ocean Engineering, 2008, 35 (2): 271−280.
[18] GARSON G D. Interpreting neural-network connection weights [J]. AI Expet, 1991, 6 (4): 46−51.

基于BP神经网络的I型金属夹芯板极限强度预测

卫钰汶，仲强，王德禹*
上海交通大学 海洋工程国家重点实验室，上海 200240

摘　要：［**目的**］针对过去对I型金属夹芯板的极限强度评估不完善的问题，提出一种采用BP人工神经网络的方法来定量确定各相关参数对I型金属夹芯板极限强度的影响。［**方法**］首先，采用非线性有限元法研究I型金属夹芯板在面内轴向压缩载荷条件下的极限强度；然后，构造BP神经网络以对不同面板柔度系数β_p、腹板柔度系数β_w和梁柱柔度系数λ下I型金属夹芯板的极限强度进行预测；最后，提出采用人工神经网络权值和偏置法预测I型金属夹芯板极限强度的公式。［**结果**］针对所计算的算例尺寸，显示采用BP神经网络方法的极限强度预测的均方差MSE和相关系数R分别为0.001 2和0.981 8，所构建的神经网络模型具有较好的预测精度，最大误差不超过10%。［**结论**］所得结论可为I型金属夹芯板在船体结构中的应用提供参考。

关键词：I型金属夹芯板；BP人工神经网络；极限强度；非线性有限元法；预测